AMERICAN SOCIETY FOR MICROBIOLOGY | Journal of Virology

ESCRT-0 Component Hrs Promotes Macropinocytosis of Kaposi's Sarcoma-Associated Herpesvirus in Human Dermal Microvascular Endothelial Cells

Mohanan Valiya Veettil, Binod Kumar, Mairaj Ahmed Ansari, Dipanjan Dutta, Jawed Iqbal, Olsi Gjyshi, Virginie Bottero, Bala Chandran

H. M. Bligh Cancer Research Laboratories, Department of Microbiology and Immunology, Chicago Medical School, Rosalind Franklin University of Medicine and Science, North Chicago, Illinois, USA

ABSTRACT

Kaposi's sarcoma-associated herpesvirus (KSHV) enters human dermal microvascular endothelial cells (HMVEC-d), its natural *in vivo* target cells, by lipid raft-dependent macropinocytosis. The internalized viral envelope fuses with the macropinocytic membrane, and released capsid is transported to the nuclear vicinity, resulting in the nuclear entry of viral DNA. The endosomal sorting complexes required for transport (ESCRT) proteins, which include ESCRT-0, -I, -II, and -III, play a central role in endosomal trafficking and sorting of internalized and ubiquitinated receptors. Here, we examined the role of ESCRT-0 component Hrs (hepatocyte growth factor-regulated tyrosine kinase substrate) in KSHV entry into HMVEC-d by macropinocytosis. Knockdown of Hrs by short hairpin RNA (shRNA) transduction resulted in significant decreases in KSHV entry and viral gene expression. Immunofluorescence analysis (IFA) and plasma membrane isolation and proximity ligation assay (PLA) demonstrated the translocation of Hrs from the cytosol to the plasma membrane of infected cells and association with α-actinin-4. In addition, infection induced the plasma membrane translocation and activation of the serine/threonine kinase ROCK1, a downstream target of the RhoA GTPase. Hrs knockdown reduced these associations, suggesting that the recruitment of ROCK1 is an Hrs-mediated event. Interaction between Hrs and ROCK1 is essential for the ROCK1-induced phosphorylation of NHE1 (Na^+/H^+ exchanger 1), which is involved in the regulation of intracellular pH. Thus, our studies demonstrate the plasma membrane association of ESCRT protein Hrs during macropinocytosis and suggest that KSHV entry requires both Hrs- and ROCK1-dependent mechanisms and that ROCK1-mediated phosphorylation of NHE1 and pH change is an essential event required for the macropinocytosis of KSHV.

IMPORTANCE

Macropinocytosis is the major entry pathway of KSHV in human dermal microvascular endothelial cells, the natural target cells of KSHV. Although the role of ESCRT protein Hrs has been extensively studied with respect to endosomal movement and sorting of ubiquitinated proteins into lysosomes, its function in macropinocytosis is not known. In the present study, we demonstrate for the first time that upon KSHV infection, the endogenous Hrs localizes to the plasma membrane and the membrane-associated Hrs facilitates assembly of signaling molecules, macropinocytosis, and virus entry. Hrs recruits ROCK1 to the membrane, which is required for the activation of NHE1 and an increase in submembranous intracellular pH occurring during macropinocytosis. These studies demonstrate that the localization of Hrs from the cytosol to the plasma membrane is important for coupling membrane dynamics to the cytosolic signaling events during macropinocytosis of KSHV.

Kaposi's sarcoma-associated herpesvirus (KSHV) entry into its *in vitro* adherent target cells is a multistage process which involves binding of viral glycoproteins to cell surface heparan sulfate receptors followed by interaction with specific entry receptors, induction of cell signaling pathways, and endocytosis. KSHV exploits multiple host cell surface receptors, including integrins α3β1, αVβ3, αVβ5, and α9β1 and nonintegrins CD98/xCT and EphA2, to enter the adherent target cells such as human dermal microvascular endothelial cells (HMVEC-d) and human foreskin fibroblast (HFF) cells (1–6). The interaction of KSHV with its specific entry receptors leads to the formation of a multimolecular receptor complex consisting of integrins, xCT, and EphA2 (2, 4, 7). Receptor engagement and multimolecular receptor complex formation result in autophosphorylation of focal adhesion kinase (FAK) and activation of Src, phosphatidylinositol 3-kinase (PI3-K), and Rho GTPases, and all of these molecules are targeted to specific entry sites on the plasma membrane (8–10). Our previous studies have demonstrated that the signal transduction pathways induced by KSHV and the consequent activation of their downstream molecules play a central role in coordinating the actin dynamics and the membrane protein assembly required for the successful entry of the virus into the cytoplasm (8–10). The

Received 22 October 2015 **Accepted** 21 January 2016

Accepted manuscript posted online 27 January 2016

Citation Veettil MV, Kumar B, Ansari MA, Dutta D, Iqbal J, Gjyshi O, Bottero V, Chandran B. 2016. ESCRT-0 component Hrs promotes macropinocytosis of Kaposi's sarcoma-associated herpesvirus in human dermal microvascular endothelial cells. J Virol 90:3860–3872. doi:10.1128/JVI.02704-15.

Editor: R. M. Longnecker

Address correspondence to Mohanan Valiya Veettil, mohanan.veettil@rosalindfranklin.edu.

endocytosed viral particles are then transported toward the nuclear periphery along the microtubules by utilizing dynein motor proteins to deliver their DNA content into the nucleus (11).

KSHV utilizes different endocytic pathways to enter different cell types (12–17). In HFF cells, primary B cells, and 293 cells, clathrin-dependent endocytosis is the predominant pathway of entry (12–14), whereas in HMVEC-d, entry occurs by bleb-associated macropinocytosis (15, 16, 18). Bleb-associated macropinocytosis begins with a remarkable set of events, including the formation of blebs, actomyosin contraction, bleb retraction, macropinosome formation, and eventually virus entry (18). Our studies have established that the adaptor protein c-Cbl and its interaction with myosin IIA light chain (MLC) play a significant role in blebbing and that myosin IIA is required for both actomyosin contraction and retraction of the bleb (18). Our subsequent studies proved that c-Cbl is also required for both translocation of the receptors into the lipid raft and ubiquitination of the α3β1 and αVβ3 receptors, which are critical determinants of the macropinocytic entry, trafficking, and productive infection of KSHV (19).

Ubiquitination of receptors and the adaptor proteins such as c-Cbl serves to facilitate the endocytosis of receptors and their sorting from membrane to lysosomes and subsequent degradation (20, 21). In mammalian cells, the endosomal sorting complexes required for transport (ESCRT) proteins help in sorting ubiquitinated proteins and their delivery into lysosomes. The ESCRT machinery consists of a family of four complexes, ESCRT-0, -I, -II, and -III, which sequentially assemble on the endosomal membrane. The ESCRT-0 component Hrs (hepatocyte growth factor [HGF]-regulated tyrosine kinase substrate) acts upstream from ESCRT complexes and can recruit ESCRT-I to the endosomal membranes. This complex subsequently recruits ESCRT-II and ESCRT-III complexes, two important complexes required for the sorting of ubiquitinated proteins into late endosomes (22–25).

The Hrs protein contains several domains: an N-terminal VHS domain (Vps27p, Hrs, STAM), an FYVE domain, an ubiquitin-interacting motif, a proline-rich domain, two coiled-coil domains, and a C-terminal clathrin binding domain (26). The functional roles of the different domains of Hrs include protein-protein interaction, cellular localization, cargo sorting, and endosome motility (24, 25, 27, 28). Although the function of Hrs in intracellular trafficking and signal transduction is well established, its role in macropinocytosis remains unclear. In the present study, we provide evidence that Hrs is recruited to the plasma membrane early during KSHV infection, which is required for the virus entry by macropinocytosis. Interestingly, we found that Hrs interacts with the Rho-associated protein kinase ROCK1, which in turn activates MLC and the intracellular pH-regulating protein NHE1 to promote actomyosin contraction and intracellular pH changes required for macropinocytosis.

MATERIALS AND METHODS

Cells and virus. Primary human dermal microvascular endothelial cells (HMVEC-d CC-2543; Clonetics, Walkersville, MD) were grown in EBM2 medium with growth factors (Cambrex, Walkersville, MD). BCBL-1 cell culture, supernatant collection after tetradecanoyl phorbol acetate (TPA) induction, and virus purification procedures were performed as described previously (1). The isolation of KSHV DNA from the virus and the determination of viral copy numbers by real-time DNA PCR using KSHV ORF73 gene-specific primers were performed as previously described (29). All infections were carried out with a multiplicity of infection (MOI) of 20 DNA copies of KSHV per cell unless stated otherwise.

Antibodies and reagents. Antibodies and reagents used for this study included the following: anti-ROCK1 rabbit monoclonal antibody, anti-phospho-MLC rabbit polyclonal antibody, and anti-Na, K-ATPase rabbit polyclonal antibody (Cell Signaling Technology); anti-Hrs rabbit polyclonal antibody (Sigma); anti-NHE1 mouse monoclonal antibody (Santa Cruz); anticalnexin rabbit monoclonal antibody and mouse antiphosphoserine antibody (Abcam); anti-α-actinin-4 rabbit monoclonal antibody (Millipore); rabbit anti-gB and mouse anti-gpK8.1A antibodies created in B. Chandran's laboratory (30, 31); anti-rabbit and anti-mouse antibodies linked to horseradish peroxidase (HRP) (KPL Inc., Gaithersburg, Md.); Texas Red-conjugated dextran, Alexa 594-conjugated phalloidin, and anti-rabbit and anti-mouse secondary antibodies conjugated to Alexa 488 or Alexa 594 (Invitrogen); and protein A- and G-Sepharose CL-4B beads (Amersham Pharmacia Biotech, Piscataway, NJ).

Hrs shRNA knockdown. For short hairpin RNA (shRNA) knockdown of Hrs, five sets of bacterial glycerol stock Hrs shRNA plasmid vectors (TRCN00000037894, -37895, -37896, -37897, and -37898) were purchased from Thermo Scientific. The Hrs shRNA lentiviral plasmids were purified from the bacterial cultures (Invitrogen), and the lentiviral particles were produced by transfection with a four-plasmid system, as previously described (32). Briefly, HEK 293T cells were transiently transfected with shRNA lentiviral constructs and the plasmid packaging system (Gag-Pol, Rev, and vesicular stomatitis virus G [VSV-G]), and the supernatants were collected and filtered. The lentiviral particles produced from each plasmid vector were tested for knockdown efficiency by Western blotting. We found that TRCN00000037897 and TRCN00000037898 had the highest knockdown efficiency among the five shRNAs. Therefore, we used Hrs shRNAs created with these two plasmids (Hrs shRNA1 and Hrs shRNA2) for the experiments described in this article. We used Hrs shRNA1 for all experiments except those for Fig. 1A and B, where we used both Hrs shRNA1 and -2. For a negative control, a nontargeting shRNA lentiviral pool was used.

Western blotting. Cells lysates were prepared in radioimmunoprecipitation assay (RIPA) lysis buffer (15 mM NaCl, 1 mM $MgCl_2$, 1 mM $MnCl_2$, 2 mM $CaCl_2$, 2 mM phenylmethylsulfonyl fluoride, and protease inhibitor mixture) (Sigma). The lysates were centrifuged at 12,000 rpm for 15 min at 4°C, and the protein concentration was measured with bicinchoninic acid (BCA) reagent. Equal amounts of proteins from each sample were separated by SDS-PAGE and transferred to nitrocellulose membranes. Membranes were probed with the indicated primary antibodies and detected by incubation with species-specific HRP-conjugated secondary antibodies. Immunoreactive protein bands were visualized and imaged with an enhanced-chemiluminescence HRP substrate kit (Pierce, Rockford, IL). The bands were scanned, and densitometric quantification was performed using the FluorChem FC2 and Alpha-Imager systems (Alpha Innotech Corporation, San Leonardo, CA).

Immunoprecipitation. Cell lysates were immunoprecipitated for 2 h with appropriate antibodies, and the immune complexes were captured by protein A- or G-Sepharose. The immune complexes were then eluted in sample buffer for SDS-PAGE, run on 10% gels, and transferred to membranes. The membranes were tested by Western blotting with specific primary and secondary antibodies.

Immunofluorescence microscopy. Cells grown in 8-well chamber slides were fixed with 4% paraformaldehyde after infection and permeabilized with 0.2% Triton X-100. The cells were blocked with Image-iT FX signal enhancer (Invitrogen) for 20 min and then incubated with primary antibodies against the specific proteins and subsequently stained with secondary antibodies conjugated to Alexa 488 or 594. The stained cells were mounted in mounting medium with DAPI (4′,6′-diamidino-2-phenylindole) (Invitrogen) and visualized with a Nikon 80i fluorescence microscope equipped with Metamorph digital imaging software.

PLA. Proximity ligation assay (PLA) was performed using the Duolink *in situ* detection kit (Sigma) as per the manufacturer's instructions (33, 34). Briefly, uninfected and infected cells were fixed with 4% paraformaldehyde solution for 15 min, permeabilized with Triton X-100 for 5 min,

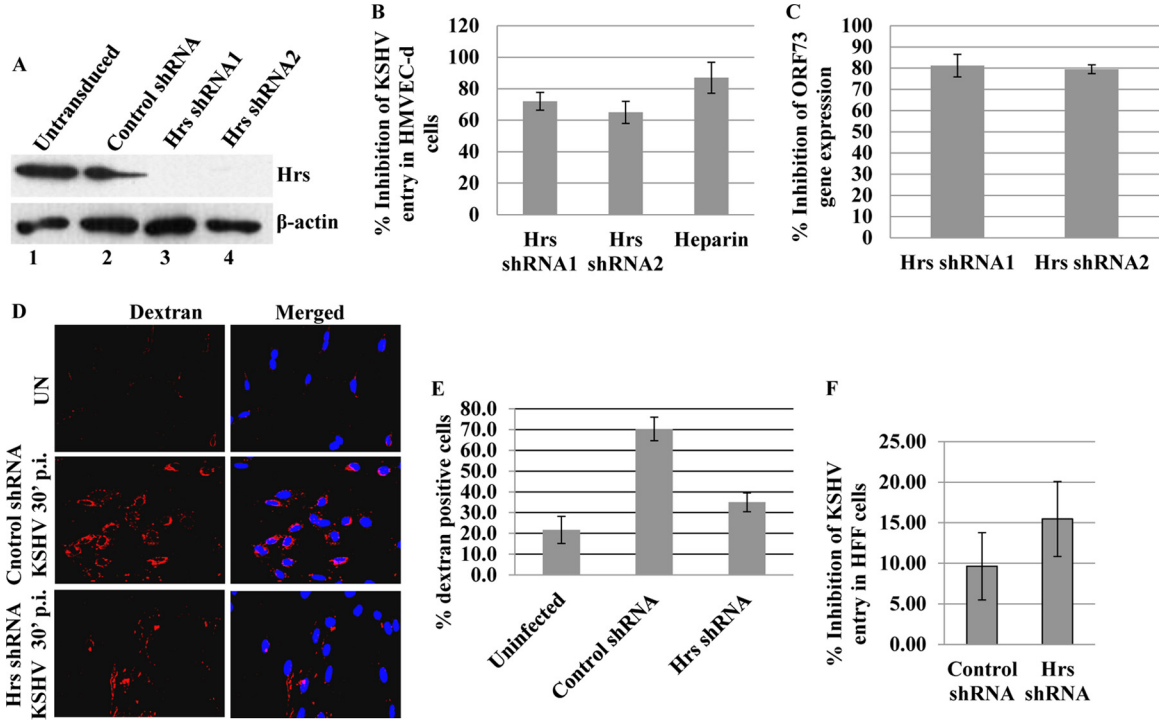

FIG 1 Effect of Hrs knockdown on KSHV entry and gene expression. (A) HMVEC-d transduced with control lentiviral shRNA or with two different lentiviral Hrs shRNAs (Hrs shRNA1 and -2) were cultured for 48 h, and the cell lysates were immunoblotted with anti-Hrs or anti-β-actin antibodies. (B) Control and Hrs shRNA-transduced HMVEC-d were infected with KSHV at an MOI of 20 of for 2 h, DNA was isolated, and the entry of KSHV was determined by real-time DNA PCR for the ORF73 gene. KSHV preincubated with heparin (100 μg/ml) for 1 h at 37°C before addition to the cells was used as control. (C) Control and Hrs shRNA-transduced HMVEC-d were infected with KSHV at an MOI of 20 for 24 h, total RNA was isolated, and viral gene expression was determined by real-time RT-PCR with KSHV ORF73 gene-specific primers and TaqMan probes. The gene expression was normalized to the expression of GAPDH. In panels B and C, data are presented as mean ± standard deviation (SD) for three independent experiments. Percent inhibition of KSHV entry was calculated as the percentage of entry with respect to the control shRNA groups. (D) Effect of Hrs knockdown on dextran uptake. Control and Hrs shRNA-transduced HMVEC-d were incubated with Texas Red-dextran in the presence or absence of KSHV (MOI of 20) for 30 min, fixed, and analyzed by immunofluorescence. DAPI was used for nuclear staining. Magnification, ×20. (E) Entry of KSHV in Hrs knockdown HFF cells. HFF cells were left untransduced or transduced with control or lentiviral Hrs shRNA for 48 h. The cells were then infected with KSHV at an MOI of 20 for 2 h, DNA was isolated, and the entry of KSHV was determined by real-time DNA PCR for the ORF73 gene. Data represent the mean ± SD. Percent inhibition of entry was calculated compared to untransduced cells.

washed with phosphate-buffered saline (PBS), and incubated for 1 h with the Duolink blocking buffer. The cells were then incubated with pairs of primary antibodies in Duolink antibody diluent solution and then labeled with Duolink PLA Plus and Minus probes for 1 h at 37°C. This was followed by hybridization, ligation, amplification, and detection using a red fluorescent probe. The red fluorescent fluorophore-tagged oligonucleotides were visualized using a Nikon Eclipse 80i microscope equipped with Metamorph digital imaging software.

Determination of KSHV entry by real-time DNA PCR. Target cells were infected with KSHV at an MOI of 20 at 37°C for 2 h. After infection, the cells were washed with Hanks balanced salt solution (HBSS) and treated with 0.25% trypsin-EDTA for 5 min at 37°C to remove the bound but noninternalized virus. Total DNA was isolated from the uninfected and infected cells using a DNeasy kit (Qiagen, Valencia, CA), and real-time DNA PCR was carried out using primer sets described previously (29). To calculate the percent inhibition of KSHV entry, internalized KSHV DNA was quantitated by amplification of the ORF73 gene by real-time DNA PCR. The KSHV ORF73 gene cloned in the pGEM-T vector (Promega) was used for the external standard.

Determination of KSHV gene expression by real-time RT-PCR. Isolation of total RNA from cells, reverse transcription, and quantitative PCR (qPCR) analysis were carried out using primer sets described previously. Briefly, total RNA was isolated from the lysate using the RNeasy kit (Qiagen) and quantified, and the ORF73 expression was detected by real-time reverse transcription-PCR (RT-PCR) using specific primers and TaqMan probes (29). GAPDH (glyceraldehyde-3-phosphate dehydrogenase) gene expression was used to normalize the expression levels of ORF73.

Isolation of membrane fraction. Subcellular fractionation and cell membrane preparation were performed as described previously (18, 35). Briefly, cells were homogenized with a Dounce homogenizer in homogenization buffer (250 mM sucrose, 20 mM HEPES, 10 mM KCl, 1 mM EDTA, 1 mM EGTA, and protease inhibitors). The homogenate was centrifuged at 3,000 rpm for 5 min, and the postnuclear supernatant was centrifuged at 8,000 rpm for 5 min at 4°C. The supernatant was again centrifuged at 40,000 rpm for 1 h at 4°C, and the cytosolic (supernatant) and membrane (pellet) fractions were separated. The membrane fractions were lysed in radioimmunoprecipitation assay (RIPA) buffer and used for Western blotting.

Analysis of dextran uptake. For the dextran uptake study, HMVEC-d were incubated with Texas Red-labeled dextran (40 kDa, 0.5 mg/ml; Invitrogen) and KSHV for 30 min. The cells were then washed twice in HBSS, fixed with 4% paraformaldehyde for 15 min, and washed three times with PBS. Internalized dextran was observed under an immunofluorescence microscope.

To perform quantitative analysis of dextran uptake, the dextran-positive cells were counted under the immunofluorescence microscope. At least 10 different microscopic fields of 25 to 30 cells each were counted for each experiment and the results displayed as percentage of dextran-positive cells.

Intracellular pH measurement. An equal number of cells in 96-well plates were loaded with BCECF-AM [bis-(2-carboxy-ethyl)-5-(and-6)-carboxyfluorescein, acetoxy-methyl) (10 μM) in HBSS for 30 min. The cells were washed with HBSS to remove the free dye and then infected with KSHV for 2, 5, and 10 min at 37°C. Immediately after infection, BCECF fluorescence was excited with a 485/20 filter, and the emission was measured with a 528/20 filter on a BioTek Synergy2 HT microplate reader. The average readings for each time point were calculated and the changes in pH expressed as relative fluorescent units.

Statistical analyses. Statistical significance was calculated using a two-tailed Student *t* test. A *P* value of <0.05 was considered significant.

RESULTS

Hrs knockdown inhibits KSHV entry and gene expression in HMVEC-d. To explore the role of Hrs in KSHV infection, we performed Hrs knockdown in HMVEC-d using two different lentiviral Hrs shRNAs (Hrs shRNA1 and -2). HMVEC-d were transduced with control and Hrs shRNAs, and the efficiency of knockdown was determined 48 h after transduction by Western blotting with anti-Hrs antibody. As shown in Fig. 1A, both the Hrs shRNA1 and Hrs shRNA2 completely knocked down endogenous Hrs expression. To address whether Hrs inhibition affects the entry of KSHV, control and Hrs shRNA-transduced HMVEC-d were infected with KSHV for 2 h, DNA was isolated, and the internalized viral DNA copy numbers were determined by measuring viral ORF73 DNA copy numbers by real-time DNA PCR. Compared to that in the control shRNA-transduced cells (copy number, 18,009 ± 938), the entry of KSHV was significantly reduced (~65 to 70%) in both Hrs shRNA1 (4,427 ± 49) and Hrs shRNA2 (5,330 ± 214) knockdown cells. Heparin-treated virus, which cannot bind and enter the cells, was used as a control (Fig. 1B). We next investigated whether Hrs knockdown also results in decreased viral gene expression. Control and Hrs shRNA-transduced HMVEC-d were infected with KSHV for 24 h, and viral gene expression of the latency-associated ORF73 gene was determined by real-time RT-PCR analysis. Similar to the entry results, the expression of the ORF73 gene in both Hrs shRNA1 (copy number, 7,742 ± 2,180)- and shRNA2 (8,364 ± 963)-transduced cells was reduced compared to that in control cells (41,135 ± 680). Hrs shRNA-transduced cells showed 70 to 80% inhibition of ORF73 gene expression (Fig. 1C), suggesting that the decreased viral entry results in decreased gene expression in Hrs knockdown cells.

Since macropinocytosis is the major pathway of KSHV entry leading to a productive infection in HMVEC-d (16, 18), we asked whether the decreased entry in Hrs shRNA-transduced cells is correlated with macropinocytosis. The macropinocytosis of KSHV in the control and Hrs shRNA-transduced cells was assessed by incubating the cells with the macropinocytosis marker dextran (Texas Red labeled) in the presence or absence of virus for 30 min. Compared to that in the uninfected cells, KSHV infection resulted in a considerable increase in dextran uptake in the control shRNA-transduced cells (Fig. 1D, upper and middle panels). However, Hrs shRNA-transduced cells incubated with dextran and KSHV showed a substantial decrease in dextran uptake compared to the control shRNA-transduced cells (Fig. 1D, middle and lower panels). Quantitative analysis performed by counting the number of dextran-positive cells in the control and Hrs shRNA-transduced cells confirmed the decreased dextran uptake in Hrs shRNA-transduced cells (Fig. 1E). This result suggested that Hrs plays a role in macropinocytosis-mediated entry of KSHV into endothelial cells.

In addition to macropinocytic mode of entry in endothelial cells, KSHV is known to enter by clathrin-mediated endocytosis in other target cells, such as HFF, HEK293, and B cells. To assess whether Hrs is involved in clathrin-mediated endocytosis of KSHV, we examined the effect of Hrs knockdown on the entry of KSHV in HFF cells (Fig. 1.F). HFF cells transduced with control or lentiviral Hrs shRNA were infected with KSHV for 2 h, and the entry of KSHV was determined by measuring viral ORF73 DNA copy numbers by real-time DNA PCR. Interestingly, real-time PCR analysis demonstrated that Hrs knockdown had no significant effect on the entry of virus in HFF cells (Fig. 1F). These results suggest that Hrs plays a specific role in regulating macropinocytosis-mediated entry of KSHV but not in clathrin-mediated entry.

Hrs localizes to the plasma membrane of KSHV-infected cells. To ascertain the mechanism of Hrs function in the entry process of KSHV, we next analyzed the cellular localization of endogenous Hrs protein in the infected cells by immunofluorescent labeling. HMVEC-d were infected with KSHV for 5, 10, and 30 min and then stained for the KSHV envelope glycoprotein gB and host Hrs protein. As shown in Fig. 2A, Hrs was distributed throughout the cytoplasm in the uninfected cells. In contrast, at 5 and 10 min post-KSHV infection, Hrs localized predominantly in the plasma membranes (Fig. 2A, arrowheads), and the KSHV gB staining (Fig. 2A, block arrows) was also observed in similar regions of the infected cell membrane. After 10 and 30 min of infection, in addition to membrane staining, we observed cytoplasmic staining as well as colocalization of Hrs with KSHV-gB in the infected cells (Fig. 2A, yellow spots).

To confirm the membrane localization of Hrs in the infected cells, plasma membranes were isolated from uninfected and infected cells and tested for the presence of Hrs using a specific anti-Hrs antibody. As shown in Fig. 2B, top panel, lanes 1 to 5, detection of Hrs in the plasma membrane fractions confirmed the membrane localization with a pattern similar to that of the immunofluorescence results in Fig. 2A. However, in the cells infected with heparin-treated KSHV, which cannot bind and enter the cells (36), we did not observe the induction of membrane translocation (Fig. 2B, lane 6). This indicates that KSHV binding and interaction with receptors are essential for the translocation of Hrs to the membrane. The purity of the membrane fraction was assessed by the detection of membrane-positive marker Na, K-ATPase in the purified membrane fractions (Fig. 2B, second panel). Additionally, the absence of the endoplasmic reticulum (ER) membrane marker calnexin by Western blotting indicated that the fraction was not contaminated with the internal membrane proteins (Fig. 2B, third panel). Western blotting of whole-cell lysate using Hrs antibody showed no variation in the total Hrs protein level (Fig. 2B, bottom panel). The recruitment of Hrs to the plasma membrane of the infected cells indicated that Hrs may be involved in the initial stages of macropinosome formation and cytoplasmic entry of the virus.

To further evaluate whether Hrs affects the cytoplasmic entry of KSHV, we examined the localization of viral particles in control and Hrs shRNA-transduced cells. Cells infected with KSHV for 30 min were stained with rhodamine-phalloidin for filamentous actin and KSHV gB to visualize the localization of KSHV. In control cells infected with KSHV, virus particles were detected at the nuclear periphery by 30 min postinfection (p.i.), whereas in Hrs

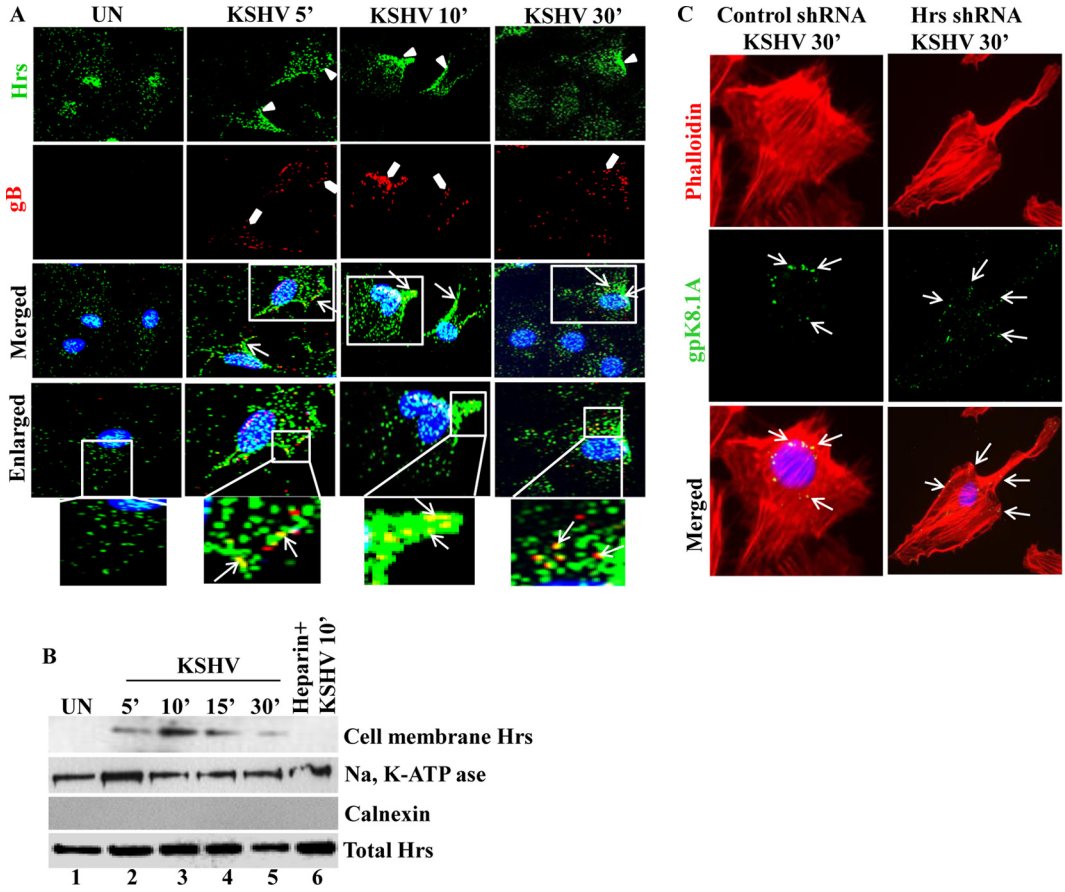

FIG 2 Localization of Hrs from the cytoplasm to the plasma membrane in KSHV-infected cells. (A) HMVEC-d left uninfected (UN) or infected with KSHV at an MOI of 20 for 5, 10, and 30 min were fixed and incubated with anti-Hrs and anti-KSHV gB antibodies, followed by staining with secondary antibodies conjugated to either Alexa 488 (green) or Alexa 594 (red). The boxed regions are enlarged below the images. Arrowheads indicate Hrs membrane localization, block arrows indicate gB staining, and white arrows indicate Hrs and gB localization at different time points of infection. Magnification, ×40. (B) HMVEC-d infected with KSHV (MOI of 20) for the indicated times were fractionated into membrane and cytosolic fractions. The membrane fractions were Western blotted with antibodies specific to Hrs, plasma membrane marker Na, K-ATPase, and endoplasmic reticulum (ER) marker calnexin. The bottom panel shows Western blotting of total cell lysate with anti-Hrs antibody. (C) Localization of KSHV in control and Hrs knockdown HMVEC-d. Control and Hrs shRNA-transduced HMVEC-d infected with KSHV for 30 min were subjected to immunofluorescence microscopy using anti-gpK8.1A (viral envelope glycoprotein) antibody for the detection of KSHV and rhodamine phalloidin for F-actin staining. DAPI was used for nuclear staining. Arrows indicate areas where KSHV gpK8.1A staining was observed. Magnification, ×80.

shRNA-transduced cells, the virus particles failed to enter the cells and were found stuck at the cell surface (Fig. 2C). This result indicated that there is a significant correlation between the membrane recruitment of Hrs and the early stages of KSHV entry by macropinocytosis.

Hrs localizes to the membrane by interacting with α-actinin-4 in the infected cells. Macropinocytosis is an actin-driven process that depends on actin polymerization and membrane ruffling (37). As membrane-associated Hrs affects the macropinocytosis of KSHV, we rationalized that membrane localization may be achieved through the interaction of Hrs with an actin binding protein that is localized to the plasma membrane. It has been shown that Hrs is a binding partner of α-actinin-4 (38), a cytoskeleton scaffolding protein that transiently associates with macropinosomes (39). Moreover, we have reported before that α-actinin-4 formed a complex with the membrane-associated proteins EphA2, myosin IIA, and CIB1 in KSHV-infected cells (15). Since α-actinin-4 primarily cross-links F-actin and forms an α-actinin-4–F-actin network surrounding macropinosomes, we hypothesized that the interaction of α-actinin-4 with Hrs may localize Hrs to the membrane and influence macropinosome formation. To test this hypothesis, we first determined whether KSHV infection results in the recruitment of α-actinin-4 to the membrane of infected cells. Immunofluorescence analysis of uninfected and KSHV-infected cells with α-actinin-4 and KSHV envelope glycoprotein gpK8.1A antibody demonstrated that the virus particles colocalize with α-actinin-4 at 10 min postinfection at the membrane of infected cells (Fig. 3A). To evaluate whether α-actinin-4 and Hrs could associate with each other at the membrane, we examined the colocalization of Hrs and α-actinin-4 in KSHV-infected cells. Immunofluorescence analysis of uninfected cells and cells infected with KSHV for 10 min demonstrated that Hrs colocalizes with α-actinin-4 at the membrane of infected cells (Fig. 3B).

To visualize that the interaction of α-actinin-4 with Hrs leads to the recruitment of Hrs to the cell membrane of infected cells, we used a proximity ligation assay (PLA) with antibodies against Hrs and α-actinin-4. PLA enables the identification of the association

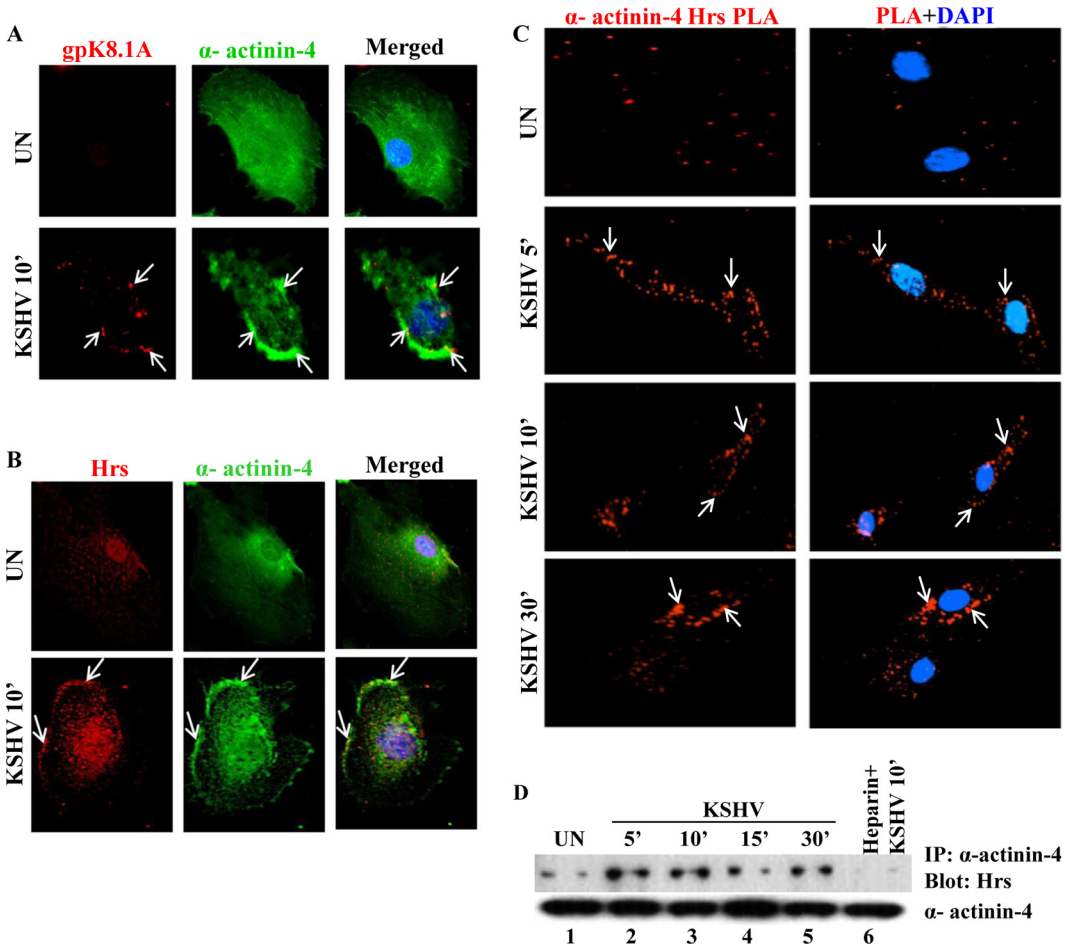

FIG 3 Translocation of Hrs to the plasma membrane is mediated by interaction with α-actinin-4. (A) Colocalization of α-actinin-4 and KSHV gpK8.1A. HMVEC-d were infected with KSHV for 10 min, and the colocalization of α-actinin-4 and KSHV gpK8.1A in the infected and uninfected cells was analyzed by costaining with anti-α-actinin-4 and anti-gpK8.1A antibodies. Arrows indicate the localization of gpK8.1A and α-actinin-4 in the infected cells. Magnification, ×80. (B) Immunofluorescence colocalization of Hrs and α-actinin-4. HMVEC-d infected with KSHV for 10 min were stained with anti-Hrs and anti-α-actinin-4 antibodies and visualized by incubation with secondary antibodies conjugated to Alexa 594 (red) or Alexa 488 (green). Colocalization of Hrs and α-actinin-4 (yellow) is indicated by arrows. Nuclei were stained with DAPI. Magnification, ×80. (C) Proximity ligation assay (PLA) showing the association of α-actinin-4 and Hrs. HMVEC-d were infected with KSHV for different times, the infected cells were fixed and incubated with anti-Hrs and anti-α-actinin-4 antibodies, and PLA was performed using oligonucleotide-conjugated PLA probes. PLA signals indicating the association between Hrs and α-actinin-4 were observed as red dots by fluorescence microscopy. Nuclear staining was performed with DAPI. Magnification, ×40. (D) HMVEC-d were infected with KSHV for 5, 10, 15, and 30 min or with heparin (100 μg/ml)-treated KSHV for 10 min. The cell lysates were then subjected to immunoprecipitation (IP) with anti-α-actinin-4 antibody followed by Western blotting with anti-Hrs antibody. The bottom panel shows the immunoprecipitated α-actinin-4 band.

between two proteins which are located in close proximity (<40 nm). PLA for α-actinin-4 and Hrs association in uninfected and KSHV-infected cells for 5, 10, and 30 min showed a notable difference between uninfected and infected conditions, with very distinct punctate fluorescent signals at the plasma membrane of infected cells, indicating that Hrs and α-actinin-4 are located in close proximity. On the other hand, in uninfected cells, we observed a few Hrs–α-actinin-4 PLA dots which were diffusely distributed in the cytoplasm (Fig. 3C). To confirm their association, we assessed the interaction between α-actinin-4 and Hrs by coimmunoprecipitation analysis. As shown in Fig. 3D, immunoprecipitation of the uninfected and infected cell lysates with anti-α-actinin-4 antibody and Western blotting with anti-Hrs antibody confirmed the increased interaction between α-actinin-4 and Hrs at 5, 10, 15, and 30 min postinfection. However, heparin-treated virus-infected cells decreased α-actinin-4 and Hrs interaction, which demonstrated the specificity of KSHV-induced interaction between these two proteins (Fig. 3D, lane 6). Based on this observation, we concluded that α-actinin-4 and Hrs are both localized to the membrane and that α-actinin-4 is the molecule linking Hrs with the plasma membrane of KSHV-infected HMVEC-d.

Hrs facilitates macropinocytosis by recruiting ROCK1 to the plasma membrane of KSHV-infected cells. To define the underlying mechanism of Hrs function in macropinocytosis, we hypothesized that the interaction between α-actinin-4 and Hrs at the plasma membrane could function by orchestrating the sequential steps involved in macropinocytosis with other cytoskeletal molecules. It has been demonstrated that during the early stages of KSHV entry, RhoA GTPase induces reorganization of the actin cytoskeleton to initiate entry by coordinating integrin-activated

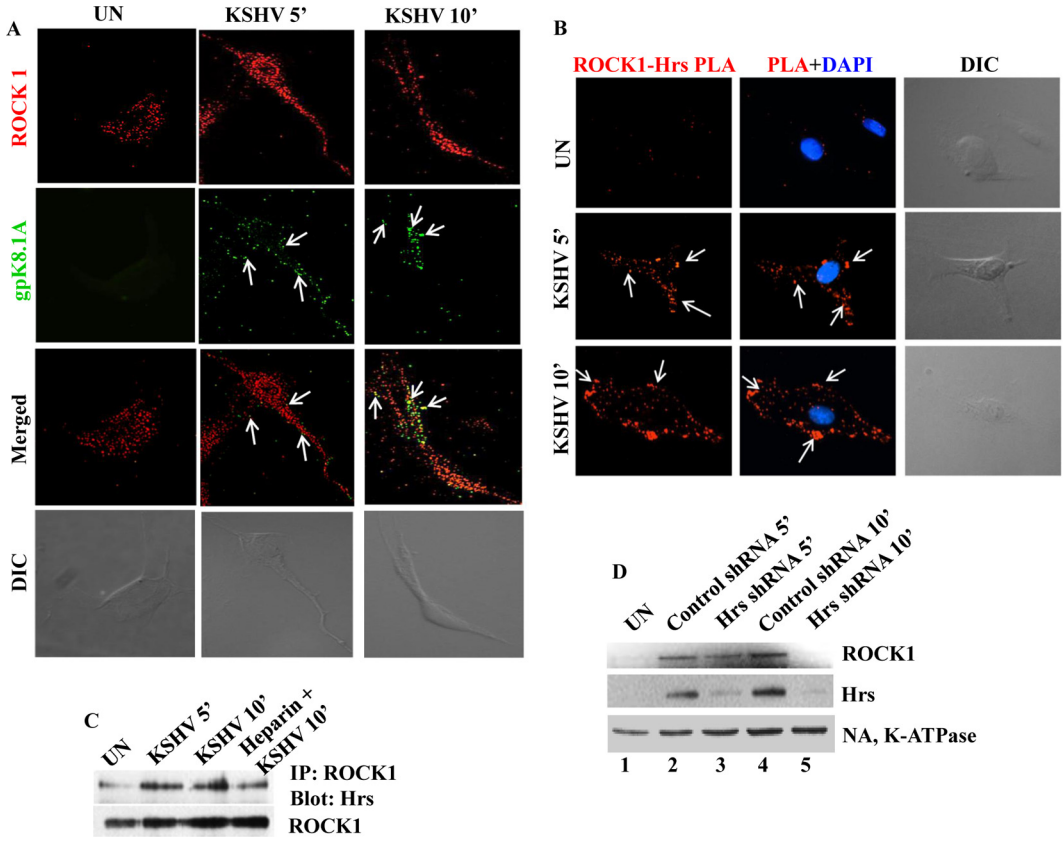

FIG 4 Hrs facilitates recruitment of ROCK1 to the plasma membrane of infected cells. (A) Membrane localization of ROCK1 in KSHV-infected cells. HMVEC-d infected with KSHV for 5 and 10 min were incubated with anti-ROCK1 and anti-KSHV gpK8.1A antibodies. Localization of ROCK1 and gpK8.1A was analyzed by staining with Alexa 488- or Alexa 594-conjugated secondary antibodies. Arrows indicate gpK8.1A and ROCK1 localization at different times of infection. The differential interference contrast (DIC) image shown in the bottom panels corresponds to the fluorescence image. Magnification, ×80. (B) Colocalization of Hrs and ROCK1 visualized by *in situ* proximity ligation assay. Uninfected and KSHV-infected cells were subjected to PLA using a mouse anti-Hrs antibody and a rabbit anti-ROCK1 antibody. Nuclei were stained with DAPI. White arrows indicate fluorescent red dots representing the interaction between ROCK1 and Hrs. The corresponding DIC images are shown in the rightmost panels. Magnification, ×80. (C) Hrs interacts with ROCK1 in KSHV-infected cells. HMVEC-d were infected with KSHV for 5 and 10 min or with heparin-treated (100 μg/ml) KSHV for 10 min, and the cell lysates were immunoprecipitated with anti-ROCK1 antibody, followed by anti-Hrs or anti-ROCK1 immunoblotting. (D) Western blot showing the membrane association of ROCK1 in control and Hrs shRNA-transduced cells. Control and Hrs shRNA-transduced cells were infected with KSHV for 5 and 10 min, and the plasma membrane fractions of uninfected and infected cells were isolated and analyzed by Western blotting with antibodies for ROCK1, Hrs, and the plasma membrane marker Na, K-ATPase.

FAK, Src, and PI3-K pathways (40). Among the various downstream members of RhoA GTPases, the serine/threonine kinase ROCK1 has been shown to play a key role in RhoA-induced actin reorganization by phosphorylating myosin light chain (MLC) (41, 42). However, it was not known whether ROCK1 localizes to the plasma membrane of KSHV-infected cells. As Hrs localization to the membrane is a critical component of macropinocytosis, we speculated that Hrs might participate in cytoskeletal reorganization and macropinocytosis, possibly by recruiting ROCK1 to the plasma membrane.

In order to test this hypothesis, we first investigated the membrane localization of ROCK1 upon KSHV infection. Uninfected cells and cells infected with KSHV for 5 and 10 min were incubated with anti-ROCK1 and anti-KSHV-gB antibodies and analyzed by immunofluorescence microscopy. Compared to the cytoplasmic distribution in the uninfected cells, the analysis of ROCK1 localization in KSHV-infected cells indicates that ROCK1 is highly localized to the membrane at 5 and 10 min postinfection (Fig. 4A). This result suggested that KSHV infection is capable of directing ROCK1 to the membrane. To examine whether Hrs regulates the membrane localization of ROCK1 upon KSHV infection, we performed proximity ligation assay. Uninfected and infected cells analyzed with PLA using anti-Hrs and anti-ROCK1 antibodies showed increased red fluorescent dots at the membranes of the cells infected with KSHV at 5 and 10 min, indicating the association of Hrs and ROCK1 at the membrane periphery (Fig. 4B). To verify the physical interaction between Hrs and ROCK1 in the infected cells, we performed a coimmunoprecipitation analysis. HMVEC-d infected with KSHV for 5 and 10 min were immunoprecipitated with anti-Hrs antibody and Western blotted with anti-ROCK1 antibody. Immunoprecipitation of Hrs resulted in increased coprecipitation of ROCK1 at 5 and 10 min p.i. compared to that in the uninfected cells (Fig. 4C). However, the negative-control heparin-treated virus-infected cells had considerably reduced interaction of Hrs with ROCK1 (Fig. 4C), indicating the specificity of virus-induced interaction between Hrs and ROCK1.

To investigate whether Hrs is indeed responsible for the membrane localization of ROCK1, we examined the membrane localization of ROCK1 in Hrs knockdown cells infected with KSHV.

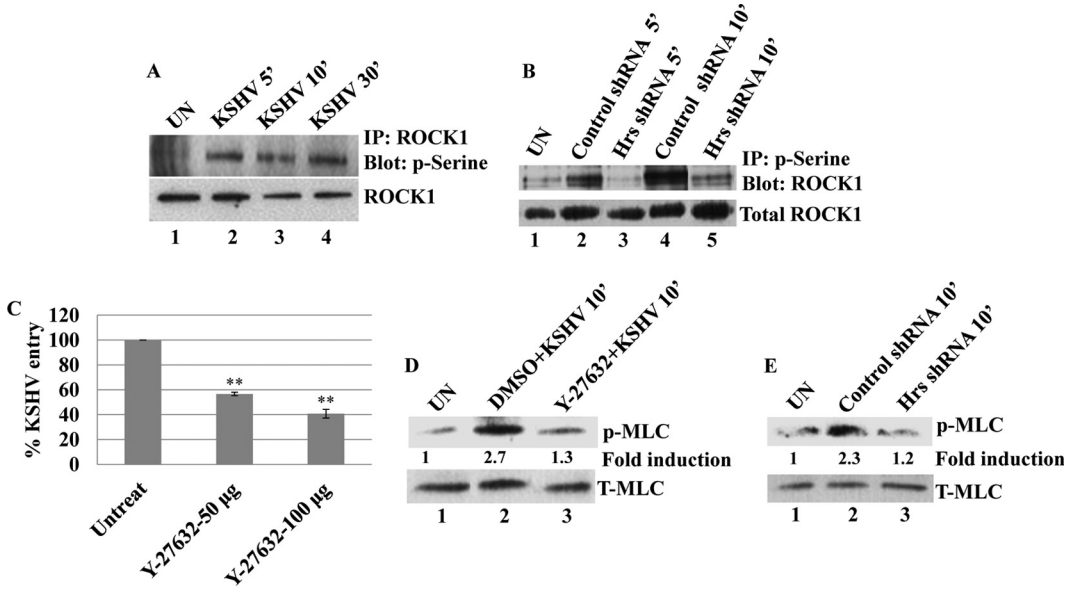

FIG 5 KSHV-induced ROCK1 plays a role in the entry of KSHV. (A) Control and Hrs shRNA-transduced HMVEC-d were infected with KSHV for 5, 10, and 30 min, and the cell lysates were subjected to immunoprecipitation with anti-ROCK1 antibodies followed by Western blotting with antiphosphoserine antibody. Total cell lysates subjected to Western blotting using anti-ROCK1 antibody were used as loading control. (B) Control and Hrs shRNA-transduced HMVEC-d were infected with KSHV for 5 and 10 min, and the cell lysates were immunoprecipitated with antiphosphoserine antibody, followed by Western blotting with an antibody against ROCK1. The bottom panel shows total cell lysates subjected to Western blotting with anti-ROCK1 antibody. (C) The ROCK1 inhibitor Y-27632 blocks the entry of KSHV. HMVEC-d pretreated with different concentrations of Y-27632 for 1 h were infected with KSHV (MOI of 20) for 2 h. Cells were harvested, total DNA was isolated, and the KSHV ORF73 copy numbers were estimated by real-time DNA PCR. Error bars represent SD for three independent experiments. **, $P < 0.001$ compared with untreated cells. (D) HMVEC-d were pretreated with either vehicle alone (DMSO) or the ROCK1 inhibitor Y-27632 for 1 h and then infected with KSHV at an MOI of 20 in the presence or absence of inhibitors. The cell lysates were blotted with antibodies against phospho-MLC (p-MLC) or total MLC (T-MLC). (E) Western blot analysis of phospho-MLC in uninfected and KSHV-infected control shRNA- and Hrs shRNA-transduced HMVEC-d. The bottom panel shows a Western blot for total MLC.

Control and Hrs knockdown cells infected with KSHV for 5 and 10 min were subjected to subcellular fractionation, and the membrane fractions were analyzed by Western blotting for ROCK1 and Hrs. As expected, ROCK1 and Hrs were present in the membrane fractions in control cells infected with KSHV (Fig. 4D, top and middle panels, lanes 2 and 4). In contrast, Hrs knockdown resulted in a considerable decrease in the recruitment of ROCK1 to the membrane (Fig. 4D, top and middle panels, lanes 3 and 5). Equal loading was verified by Western blotting with Na, K-ATPase antibody (Fig. 4D, bottom panel). This result confirmed that Hrs is crucial for the localization of ROCK1 to the plasma membrane of KSHV-infected cells.

ROCK1 promotes the entry of KSHV by phosphorylating its downstream molecule MLC. To determine the functionality of plasma membrane-associated ROCK1 in the infected cells, we examined the serine phosphorylation kinetics of ROCK1 in uninfected and KSHV-infected HMVEC-d. Compared to that in the uninfected cells, immunoprecipitation with ROCK1 and Western blotting with phosphoserine (p-serine) analysis showed increased serine phosphorylation of ROCK 1 at 5, 10, and 30 min p.i. in the infected cells (Fig. 5A, lanes 1 to 4). Since Hrs promotes the membrane association of ROCK1 in the infected cells, we next analyzed whether Hrs silencing decreases the phosphorylation of ROCK1. Control and Hrs shRNA-transduced cells were infected with KSHV for 5 and 10 min, and the cell lysates were immunoprecipitated with anti-ROCK1 antibody and blotted with p-serine antibody. As shown in Fig. 5B, Hrs knockdown resulted in considerable reduction in the phosphorylation of ROCK1 at 5 and 10 min p.i. (Fig. 5B, lanes 3 and 5) compared to the control cells (Fig. 5B, lanes 2 and 4). The increased phosphorylation of ROCK1 suggests that the downstream signaling pathways of ROCK1 are probably required for the entry of KSHV. We next determined whether the activation of ROCK1 affects the entry of KSHV. HMVEC-d were pretreated with different concentrations (50 μg/ml and 100 μg/ml) of the ROCK1-specific inhibitor Y-27632, followed by infection with KSHV for 2 h. After infection, cells were harvested, total DNA was isolated, and the entry of KSHV was determined by ORF73 gene-specific PCR. Notably, the ROCK1 inhibitor significantly blocked the entry of KSHV in a dose-dependent manner (Fig. 5C), which reinforces that the downstream signaling pathways of ROCK1 may be essential for the macropinocytosis of KSHV.

It has been demonstrated that the activation of ROCK1 is essential for equine herpesvirus 1 infection (43), and ROCK1 mediates the downstream signaling molecules by activating its immediate downstream molecule MLC (41, 42). We have previously shown that KSHV induces phosphorylation of MLC and that phosphorylated MLC is required for the actomyosin contractility that drives the process of bleb retraction and macropinocytosis of KSHV (18). To determine whether ROCK1 is required for KSHV-induced MLC phosphorylation, untreated and ROCK1-specific inhibitor Y-27632-treated HMVEC-d were infected with KSHV for 10 min, and MLC phosphorylation was determined by Western blotting. A significant decrease in MLC phosphorylation in the inhibitor-treated cells compared to the untreated cells (Fig. 5D) suggested the involvement of ROCK1-mediated MLC phosphor-

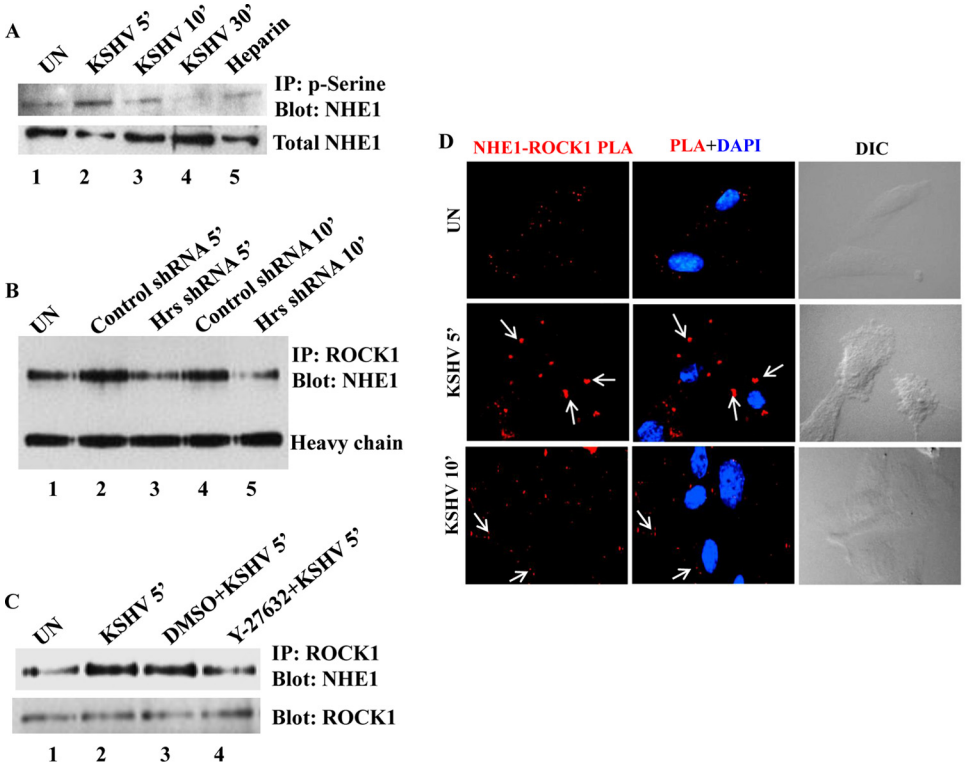

FIG 6 ROCK1 interacts with and phosphorylates NHE1 in KSHV-infected cells. (A) Kinetics of NHE1 phosphorylation in KSHV-infected cells. HMVEC-d were left uninfected or infected with KSHV at an MOI of 20 for 5, 10, and 30 min or with heparin (100 μg/ml)-treated virus for 10 min, and the cell lysates were immunoprecipitated with antiphosphoserine antibody, followed by Western blotting with anti-NHE1 antibody. The bottom panel shows total cell lysates Western blotted with anti-NHE1 antibody. (B) Control and Hrs shRNA-transduced HMVEC-d were infected with KSHV for 5 and 10 min, and the uninfected cell lysates were immunoprecipitated using anti-ROCK1 antibody, followed by Western blotting with anti-NHE1 antibody. Heavy chain is shown to verify equal loading. (C) HMVEC-d left untreated or treated with vehicle DMSO or Y-27632 for 1 h were infected with KSHV for 5 min, and the cell lysates were immunoprecipitated with anti-ROCK1 antibody and Western blotted with anti-NHE1 antibody. The bottom panel shows the membrane stripped and reprobed with anti-ROCK1. (D) PLA showing the interaction between NHE1 and ROCK1 in the membrane of blebs. Uninfected and KSHV-infected HMVEC-d were fixed, permeabilized, blocked, and probed with antibodies to Hrs and ROCK1. Interaction of Hrs and ROCK1 in the infected cells was visualized by the red fluorescence dots (white arrows) using immunofluorescence microscopy. DAPI was used for nuclear staining. Magnification, ×80.

ylation in the infected cells. As Hrs is a molecule that localizes ROCK1 to the membrane, we next examined whether Hrs regulates the phosphorylation of MLC through ROCK1. Control and Hrs shRNA-transduced cells infected with KSHV and Western blotted for p-MLC showed that in the absence of Hrs, ROCK1 was unable to promote the phosphorylation of MLC in KSHV-infected cells (Fig. 5E). These results demonstrated that the coordinated activities of the Hrs-ROCK1 interaction may play a crucial role in mediating the phosphorylation of MLC and thereby actomyosin contraction and macropinocytosis of KSHV.

Interaction of ROCK1 with NHE1 increases its phosphorylation and intracellular pH in KSHV-infected cells. Based on the above-described studies, it is clear that macropinocytosis of KSHV in HMVEC-d is characterized by Hrs-ROCK1-mediated cytoskeletal reorganization and actomyosin contraction. In addition to this, alterations in submembranous intracellular pH have been shown to be associated with macropinocytosis (44). Our previous studies have shown that the inhibition of NHE1, an Na^+/H^+ exchanger and regulator of intracellular pH, by its inhibitor ethylisopropyl amiloride (EIPA) blocked macropinocytosis of KSHV but not clathrin-mediated endocytosis (16). The inhibition of KSHV entry by EIPA reveals that intracellular pH is a key player in the regulation of macropinocytosis. It has been reported that NHE1 functions downstream of integrin receptors and a subset of membrane-associated molecules which includes RhoA and ROCK1 (45–47). Therefore, we speculated that KSHV through engagement of integrin receptors activates ROCK1 in the infected cells and that the activated ROCK1 may associate with NHE1 to increase its phosphorylation and intracellular pH required for the macropinocytosis of KSHV.

To understand the involvement of ROCK1-NHE1 function in the KSHV entry process, we first examined the serine phosphorylation of NHE1 in KSHV-infected cells. We observed that the HMVEC-d infected with KSHV exhibited a rapid but transient increase in NHE1 serine phosphorylation at 5 and 10 min, which returned to basal levels by 30 min p.i. (Fig. 6A, lanes 2 to 4). Cells infected for 10 min with heparin (100 μg/ml)-treated KSHV were used as negative control (Fig. 6A, lane 5). These data provide the evidence that signaling through ROCK1 might stimulate the phosphorylation of NHE1 in the infected cells. To investigate the involvement of Hrs in ROCK1-mediated activation of NHE1, we analyzed the interaction of ROCK1 with NHE1 in control and Hrs shRNA-transduced cells infected with KSHV. Immunoprecipitation of the cell lysates with ROCK1 and Western blotting with NHE1 showed that NHE1 coimmunoprecipitated with ROCK1 in both control and Hrs shRNA-infected cells; however,

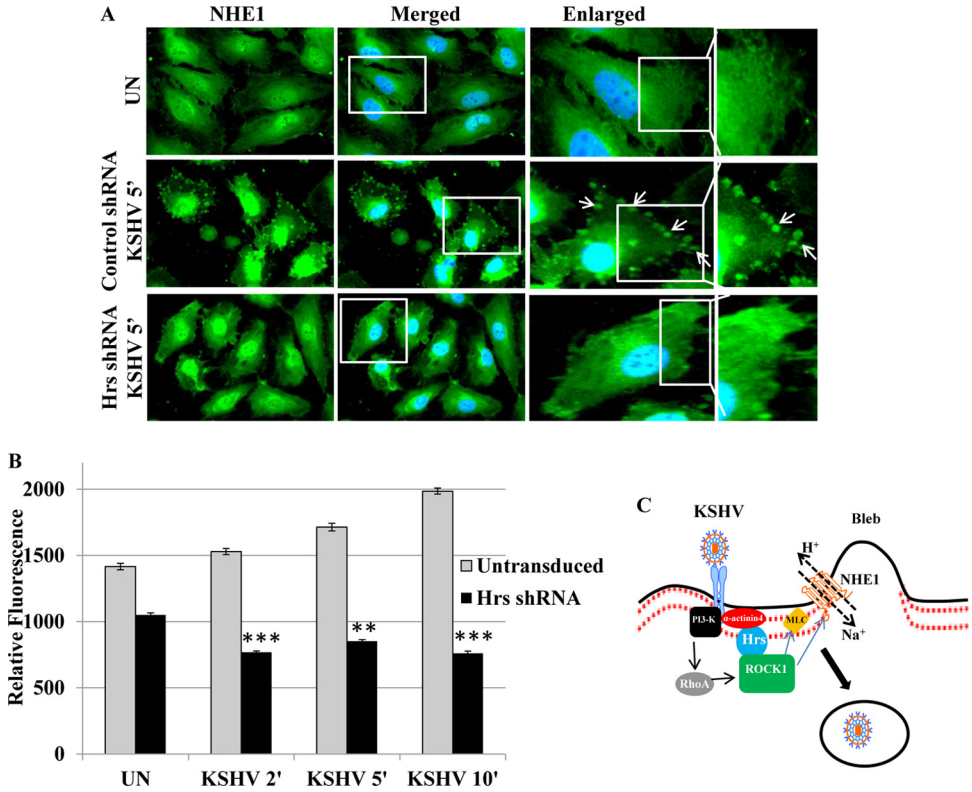

FIG 7 Hrs shRNA inhibits NHE1 association with membrane blebs and intracellular pH in the infected cells. (A) Control and Hrs shRNA-transduced HMVEC-d infected with KSHV for 5 min were incubated with anti-NHE1 antibody and observed by using Alexa 488-conjugated secondary antibody. Nuclei were stained with DAPI. The right panels are the enlarged view of the boxed areas. Arrows indicate localization of NHE1 to membrane blebs. Magnification, ×40. (B) Hrs shRNA decreases intracellular pH in the infected cells. Untransduced and Hrs shRNA-transduced cells loaded with BCECF-AM were infected with KSHV at an MOI of 20 for 2, 5, and 10 min. The intracellular pH change was detected by measuring the BCECF fluorescence using a microplate reader with excitation at 485 nm and emission at 528 nm. **, $P < 0.001$; ***, $P < 0.0001$ (compared with untransduced cells). (C) Model diagram depicting the function of Hrs in KSHV entry. KSHV infection induces the recruitment of Hrs to the membrane of infected cells via α-actinin-4, an actin cross-linking protein. The interaction of Hrs with ROCK1 during infection facilitates the membrane association of ROCK1. As was previously shown, simultaneously the interaction of KSHV with host cell surface receptors may facilitate signaling of RhoA via a PI3-K cascade. RhoA mediates the activation of ROCK1, which can contribute to phosphorylation of MLC, leading to macropinocytosis of KSHV. Concurrent interaction of ROCK1 with NHE1 and activation of NHE1 may increase the pH locally at the sites of macropinosome formation, and the increased pH may promote macropinocytosis of KSHV.

the interaction between NHE1 and ROCK1 was much more pronounced in the control cells infected with KSHV (Fig. 6B, lanes 2 and 4) than in the Hrs shRNA-infected cells (Fig. 6B, lanes 3 and 5). To verify the involvement of ROCK1 in NHE1 activation, we examined the effect of ROCK1 inhibitor on the KSHV-induced interaction between ROCK1 and NHE1. ROCK1 inhibitor treatment resulted in a weak interaction between NHE1 and ROCK1 in the infected cells compared to the untreated and dimethyl sulfoxide (DMSO) vehicle-treated cells (Fig. 6C), indicating that ROCK1 has a distinct role in regulating NHE1 activity at the membrane of KSHV-infected cells. To further analyze whether KSHV infection enhances ROCK1 and NHE1 accumulation at the membrane of blebs, proximity ligation assay was performed in HMVEC-d infected with KSHV for 5 and 10 min. Punctate red fluorescent signals indicating the association of NHE1 and ROCK1 were observed at the bleb membrane (Fig. 6D) at 5 and 10 min, suggesting the involvement of these two proteins in bleb-associated macropinocytosis.

As our studies demonstrated the simultaneous interaction of three proteins, i.e., Hrs, ROCK1, and NHE1, we next examined whether Hrs affects the localization of NHE1 and thus the regulation of pH in the infected cells. The cellular localization of endogenous NHE1 was examined by immunofluorescent labeling in control and Hrs shRNA-transduced cells infected with KSHV. In control shRNA-transduced cells, at 5 min p.i., NHE1 was detected at the membrane boundary of blebs, which is the first phase associated with bleb-associated macropinocytosis of KSHV. In contrast, NHE1 accumulation was not detected in Hrs shRNA-transduced cells (Fig. 7A). This indicates that Hrs mediates the ROCK1-NHE1 interaction and their accumulation at the blebs, which may regulate an increase in submembranous pH during macropinocytosis of KSHV. To determine whether Hrs regulates ROCK1-mediated NHE1 activation and an increase in intracellular pH, we analyzed the intracellular pH change in control and Hrs shRNA-transduced cells infected with KSHV. Control and Hrs shRNA-transduced cells were loaded with the fluorescent probe BCECF-AM, followed by infection with KSHV for 2, 5, and 10 min, and the relative fluorescence was assessed by analyzing the fluorescent signals. Our results demonstrate that the BCECF fluorescence signal was gradually increased at 2, 5, and 10 min p.i. in control cells infected with KSHV (Fig. 7B), indicating an increase in intracellular pH. However, Hrs shRNA-transduced cells in-

fected with KSHV exhibited significantly lower fluorescence signals at different time points of infection (Fig. 7B). This result suggested that Hrs is involved in triggering the NHE1-mediated pH increase in the infected cells during macropinocytosis of KSHV. Overall, our functional studies demonstrate that Hrs-mediated ROCK1 localization at the membrane not only phosphorylates MLC but is also able to associate with NHE1 to increase the submembranous intracellular pH and facilitate the macropinocytosis-mediated entry of KSHV.

DISCUSSION

Hrs, a member of the family of ESCRT proteins, plays a significant role in cargo sorting at the level of the early or late endosome and in intracellular trafficking and signal transduction (24, 25, 28, 48). Besides its cytoplasmic distribution and distinct function in endosomal transport, Hrs has been identified at the membrane of some cell types, such as T cells and macrophages (49), where macropinocytosis is a constitutively active process. However, there have been no systematic studies to determine the relationship between the events that drive the process of macropinocytosis and Hrs functions at the membrane in any system. The results of our present study for the first time show that during macropinocytosis of KSHV, Hrs localizes to the plasma membrane and the membrane-associated Hrs facilitates assembly of signaling molecules, macropinocytosis, and virus entry. Inhibition of this pathway by Hrs shRNA resulted in decreased entry and gene expression of the virus, suggesting that Hrs is a key element in the early stage of macropinocytosis of KSHV. We therefore carried out a detailed analysis of the subcellular localization and functional significance of Hrs in macropinocytosis-mediated entry of KSHV.

In endothelial cell entry, KSHV utilizes bleb-associated macropinocytosis, a unique mechanism that allows successful entry and infection of the virus (16, 18). KSHV entry is initiated by binding to the cell surface heparan sulfate receptor. After the initial attachment, the virus interacts with specific entry receptors which include integrin molecules α3β1, αVβ3, αVβ5, and α9β1, the amino acid transporter x-CT protein, and EphA2 (1–6). Interaction of KSHV with the receptors activates a sequence of intracellular signaling proteins such as FAK, Src, and PI3-K (8–10) (Fig. 7C). Phosphorylation of these proteins orchestrates membrane organization and dynamics through remodeling of cytoskeleton and thus facilitates the entry by macropinocytosis (8–10). Previous studies have reported that during macropinocytosis, PI3-K binds to α-actinin-4, forms an actinin-4–F-actin network surrounding macropinosomes, and regulates the morphological changes associated with macropinosome formation (39, 50). Our current studies showed that α-actinin-4 was able to localize Hrs to the membrane and that the recruitment of Hrs to the membrane of infected cells provides a connection between the regulators of cytoskeleton remodeling and macropinocytosis (Fig. 7C). Hrs is well known for its function in cytoplasmic transport; however, translocation of Hrs from the cytoplasm to the membrane indicates that Hrs regulates a different set of molecules and exerts different cellular functions in the context of KSHV infection. Since Hrs has multiple domains for protein-protein interaction, Hrs might form a multicomponent signaling domain and take part in macropinosome formation by linking a series of signaling pathways.

In bleb-associated macropinocytosis of KSHV, formation of blebs takes place through bulging of the plasma membrane and its retraction by forming a macropinosome which contains KSHV (18). It has been demonstrated that PI3-K activation upon KSHV infection is involved in cytoskeletal reorganization and the regulation of macropinocytosis via its downstream molecule RhoA GTPase. KSHV-dependent activation of RhoA GTPase plays active roles in cytoskeletal dynamics and clathrin-dependent endocytosis of KSHV in HEK 293 cells as well as macropinocytosis of KSHV in endothelial cells (40, 51). Signaling from RhoA to the cytoskeleton is regulated through Rho-associated protein kinase ROCK1, an important downstream effector of RhoA GTPase (52, 53). ROCK1 has been found to phosphorylate MLC and facilitate bleb retraction and macropinocytosis (54, 55). Although ROCK1 is known to be an upstream regulator of MLC phosphorylation, no direct interaction of these two proteins has been observed previously in KSHV macropinocytosis. Our finding that Hrs localizes ROCK1 to the plasma membrane and thereby leads to the RhoA-mediated activation of ROCK1 shows one of the critical events required for blebbing and bleb retraction (Fig. 7C). The localization of Hrs coincides with the accumulation of ROCK1 at the cell membrane and provides a mechanism by which Hrs and ROCK1 coordinately control bleb-associated macropinocytosis through MLC phosphorylation and actomyosin contraction. This result extends our previous findings and confirms that the activation of RhoA and the downstream components of RhoA is required for successful entry of the virus.

In addition to cytoskeletal dynamics, the process of blebbing and macropinosome formation also requires other aspects of membrane dynamics, which include an increase in submembranous pH (44). We identified that the membrane-associated ROCK1 interacts with NHE1 and that NHE1 activation increases intracellular pH, which has been suggested to promote macropinocytosis. It was previously demonstrated that the NHE1 inhibitor EIPA inhibits macropinocytosis and entry of KSHV (16). Although the effect of NHE1 inhibitor EIPA on macropinocytosis has been recognized, how the inhibitor regulates the process of macropinocytosis was not reported previously. EIPA-induced inhibition appeared to be mediated through the inhibition of Na^+/H^+ exchanger activity and altered cytosolic pH. It has been reported that during macropinocytosis, Na^+/H^+ exchanger activity increases submembranous pH and facilitates macropinocytosis (44). In agreement with that report, the results of our present study demonstrate that KSHV infection induces NHE1 activity and increases the cytosolic pH, which suggests that both macropinocytosis and entry of KSHV are regulated by NHE1. As NHE1 is a regulator of intracellular pH, a long-term activation of this molecule may lead to several unfavorable effects in the intracellular environment. A transient increase in phosphorylation for a short period in our study reveals that it exhibits a modest level of pH change required for cell surface modifications during the initial stages of macropinosome formation. Thus, we confirmed our previous findings and also established that NHE1 regulates the submembranous intracellular pH change at the plasma membrane that is essential for the macropinocytosis of KSHV, which provides further progress in our understanding of the specific role of NHE1 in KSHV macropinocytosis.

We also demonstrated that the localization of Hrs and the accumulation of ROCK1 at the cell membrane are needed for the activation of NHE1 and intracellular pH regulation during macropinocytosis. Hrs shRNA inhibited the activation of Na^+/H^+ through ROCK1, suggesting the regulatory activity of Hrs on these

two proteins. These studies suggest that Hrs is a significant component in positioning signaling molecules at the membrane and in coordinating the signal pathways to regulate the cytoskeletal and membrane dynamics during macropinocytosis. The results of the present study also show that Hrs interacts with KSHV in the cytoplasm at 30 min p.i., as evidenced by the colocalization of KSHV glycoproteins with Hrs in Fig. 2A. As Hrs plays a role in the recruitment and assembly of the ESCRT complex on the endosomal membrane (24, 25), the formation of an ESCRT complex with ESCRT-I, -II, and -III proteins may be involved in endosome movement, fusion of the virus with the endosomal membrane, or the delivery of viral DNA into the nucleus. Further studies are required to understand the interaction of Hrs with other ESCRT proteins as well as to understand how they promote the various events involved in the entry and trafficking of the virus. In conclusion, our study demonstrates that during KSHV infection, Hrs changes its subcellular distribution between the cytosol and plasma membrane, which is important for coupling membrane dynamics to the cytosolic signaling events that happen during macropinocytosis. Additionally, the localization of Hrs to the membrane and the associated activities of ROCK1 and NHE1 regulate the morphological changes and intracellular dynamics for the macropinocytic entry of KSHV.

ACKNOWLEDGMENTS

This study was supported in part by Public Health Service grant CA 168472 and the Rosalind Franklin University of Medicine and Science H. M. Bligh Cancer Research Fund to B.C.

We thank Keith Philibert for critically reading the manuscript.

FUNDING INFORMATION

HHS | NIH | National Cancer Institute (NCI) provided funding to Bala Chandran under grant numbers CA 075911 and CA168472.

REFERENCES

1. **Akula SM, Pramod NP, Wang FZ, Chandran B.** 2002. Integrin alpha3beta1 (CD 49c/29) is a cellular receptor for Kaposi's sarcoma-associated herpesvirus (KSHV/HHV-8) entry into the target cells. Cell **108:**407–419. http://dx.doi.org/10.1016/S0092-8674(02)00628-1.
2. **Veettil MV, Sadagopan S, Sharma-Walia N, Wang FZ, Raghu H, Varga L, Chandran B.** 2008. Kaposi's sarcoma-associated herpesvirus forms a multimolecular complex of integrins (alphaVbeta5, alphaVbeta3, and alpha3beta1) and CD98-xCT during infection of human dermal microvascular endothelial cells, and CD98-xCT is essential for the postentry stage of infection. J Virol **82:**12126–12144. http://dx.doi.org/10.1128/JVI.01146-08.
3. **Hahn AS, Kaufmann JK, Wies E, Naschberger E, Panteleev-Ivlev J, Schmidt K, Holzer A, Schmidt M, Chen J, Konig S, Ensser A, Myoung J, Brockmeyer NH, Sturzl M, Fleckenstein B, Neipel F.** 2012. The ephrin receptor tyrosine kinase A2 is a cellular receptor for Kaposi's sarcoma-associated herpesvirus. Nat Med **18:**961–966. http://dx.doi.org/10.1038/nm.2805.
4. **Chakraborty S, Veettil MV, Bottero V, Chandran B.** 2012. Kaposi's sarcoma-associated herpesvirus interacts with EphrinA2 receptor to amplify signaling essential for productive infection. Proc Natl Acad Sci U S A **109:**E1163–72. http://dx.doi.org/10.1073/pnas.1119592109.
5. **Walker LR, Hussein HA, Akula SM.** 2014. Disintegrin-like domain of glycoprotein B regulates Kaposi's sarcoma-associated herpesvirus infection of cells. J Gen Virol **95:**1770–1782. http://dx.doi.org/10.1099/vir.0.066829-0.
6. **Garrigues HJ, Rubinchikova YE, Dipersio CM, Rose TM.** 2008. Integrin alphaVbeta3 Binds to the RGD motif of glycoprotein B of Kaposi's sarcoma-associated herpesvirus and functions as an RGD-dependent entry receptor. J Virol **82:**1570–1580. http://dx.doi.org/10.1128/JVI.01673-07.
7. **Garrigues HJ, DeMaster LK, Rubinchikova YE, Rose TM.** 2014. KSHV attachment and entry are dependent on alphaVbeta3 integrin localized to specific cell surface microdomains and do not correlate with the presence of heparan sulfate. Virology **464-465:**118–133. http://dx.doi.org/10.1016/j.virol.2014.06.035.
8. **Chandran B.** 2010. Early events in Kaposi's sarcoma-associated herpesvirus infection of target cells. J Virol **84:**2188–2199. http://dx.doi.org/10.1128/JVI.01334-09.
9. **Veettil MV, Bandyopadhyay C, Dutta D, Chandran B.** 2014. Interaction of KSHV with host cell surface receptors and cell entry. Viruses **6:**4024–4046. http://dx.doi.org/10.3390/v6104024.
10. **Chakraborty S, Veettil MV, Chandran B.** 2012. Kaposi's sarcoma associated herpesvirus entry into target cells. Front Microbiol **3:**6. http://dx.doi.org/10.3389/fmicb.2012.00006.
11. **Naranatt PP, Krishnan HH, Smith MS, Chandran B.** 2005. Kaposi's sarcoma-associated herpesvirus modulates microtubule dynamics via RhoA-GTP-diaphanous 2 signaling and utilizes the dynein motors to deliver its DNA to the nucleus. J Virol **79:**1191–1206. http://dx.doi.org/10.1128/JVI.79.2.1191-1206.2005.
12. **Akula SM, Naranatt PP, Walia NS, Wang FZ, Fegley B, Chandran B.** 2003. Kaposi's sarcoma-associated herpesvirus (human herpesvirus 8) infection of human fibroblast cells occurs through endocytosis. J Virol **77:**7978–7990. http://dx.doi.org/10.1128/JVI.77.14.7978-7990.2003.
13. **Inoue N, Winter J, Lal RB, Offermann MK, Koyano S.** 2003. Characterization of entry mechanisms of human herpesvirus 8 by using an Rta-dependent reporter cell line. J Virol **77:**8147–8152. http://dx.doi.org/10.1128/JVI.77.14.8147-8152.2003.
14. **Rappocciolo G, Hensler HR, Jais M, Reinhart TA, Pegu A, Jenkins FJ, Rinaldo CR.** 2008. Human herpesvirus 8 infects and replicates in primary cultures of activated B lymphocytes through DC-SIGN. J Virol **82:**4793–4806. http://dx.doi.org/10.1128/JVI.01587-07.
15. **Bandyopadhyay C, Valiya-Veettil M, Dutta D, Chakraborty S, Chandran B.** 2014. CIB1 synergizes with EphrinA2 to regulate Kaposi's sarcoma-associated herpesvirus macropinocytic entry in human microvascular dermal endothelial cells. PLoS Pathog **10:**e1003941. http://dx.doi.org/10.1371/journal.ppat.1003941.
16. **Raghu H, Sharma-Walia N, Veettil MV, Sadagopan S, Chandran B.** 2009. Kaposi's sarcoma-associated herpesvirus utilizes an actin polymerization-dependent macropinocytic pathway to enter human dermal microvascular endothelial and human umbilical vein endothelial cells. J Virol **83:**4895–4911. http://dx.doi.org/10.1128/JVI.02498-08.
17. **Greene W, Gao SJ.** 2009. Actin dynamics regulate multiple endosomal steps during Kaposi's sarcoma-associated herpesvirus entry and trafficking in endothelial cells. PLoS Pathog **5:**e1000512. http://dx.doi.org/10.1371/journal.ppat.1000512.
18. **Valiya Veettil M, Sadagopan S, Kerur N, Chakraborty S, Chandran B.** 2010. Interaction of c-Cbl with myosin IIA regulates Bleb associated macropinocytosis of Kaposi's sarcoma-associated herpesvirus. PLoS Pathog **6:**e1001238. http://dx.doi.org/10.1371/journal.ppat.1001238.
19. **Chakraborty S, ValiyaVeettil M, Sadagopan S, Paudel N, Chandran B.** 2011. c-Cbl-mediated selective virus-receptor translocations into lipid rafts regulate productive Kaposi's sarcoma-associated herpesvirus infection in endothelial cells. J Virol **85:**12410–12430. http://dx.doi.org/10.1128/JVI.05953-11.
20. **Levkowitz G, Waterman H, Zamir E, Kam Z, Oved S, Langdon WY, Beguinot L, Geiger B, Yarden Y.** 1998. c-Cbl/Sli-1 regulates endocytic sorting and ubiquitination of the epidermal growth factor receptor. Genes Dev **12:**3663–3674. http://dx.doi.org/10.1101/gad.12.23.3663.
21. **Lee PS, Wang Y, Dominguez MG, Yeung YG, Murphy MA, Bowtell DD, Stanley ER.** 1999. The Cbl protooncoprotein stimulates CSF-1 receptor multiubiquitination and endocytosis, and attenuates macrophage proliferation. EMBO J **18:**3616–3628. http://dx.doi.org/10.1093/emboj/18.13.3616.
22. **Henne WM, Buchkovich NJ, Emr SD.** 2011. The ESCRT pathway. Dev Cell **21:**77–91. http://dx.doi.org/10.1016/j.devcel.2011.05.015.
23. **Schmidt O, Teis D.** 2012. The ESCRT machinery. Curr Biol **22:**R116–R20. http://dx.doi.org/10.1016/j.cub.2012.01.028.
24. **Bache KG, Brech A, Mehlum A, Stenmark H.** 2003. Hrs regulates multivesicular body formation via ESCRT recruitment to endosomes. J Cell Biol **162:**435–442. http://dx.doi.org/10.1083/jcb.200302131.
25. **Raiborg C, Stenmark H.** 2002. Hrs and endocytic sorting of ubiquitinated membrane proteins. Cell Struct Funct **27:**403–408. http://dx.doi.org/10.1247/csf.27.403.
26. **Williams RL, Urbe S.** 2007. The emerging shape of the ESCRT machinery. Nat Rev Mol Cell Biol **8:**355–368. http://dx.doi.org/10.1038/nrm2162.

27. **Raiborg C, Bache KG, Gillooly DJ, Madshus IH, Stang E, Stenmark H.** 2002. Hrs sorts ubiquitinated proteins into clathrin-coated microdomains of early endosomes. Nat Cell Biol **4:**394–398. http://dx.doi.org/10.1038/ncb791.
28. **Raiborg C, Bache KG, Mehlum A, Stenmark H.** 2001. Function of Hrs in endocytic trafficking and signalling. Biochem Soc Trans **29:**472–475. http://dx.doi.org/10.1042/bst0290472.
29. **Krishnan HH, Naranatt PP, Smith MS, Zeng L, Bloomer C, Chandran B.** 2004. Concurrent expression of latent and a limited number of lytic genes with immune modulation and antiapoptotic function by Kaposi's sarcoma-associated herpesvirus early during infection of primary endothelial and fibroblast cells and subsequent decline of lytic gene expression. J Virol **78:**3601–3620. http://dx.doi.org/10.1128/JVI.78.7.3601-3620.2004.
30. **Wang FZ, Akula SM, Sharma-Walia N, Zeng L, Chandran B.** 2003. Human herpesvirus 8 envelope glycoprotein B mediates cell adhesion via its RGD sequence. J Virol **77:**3131–3147. http://dx.doi.org/10.1128/JVI.77.5.3131-3147.2003.
31. **Zhu L, Puri V, Chandran B.** 1999. Characterization of human herpesvirus-8 K8.1A/B glycoproteins by monoclonal antibodies. Virology **262:**237–249. http://dx.doi.org/10.1006/viro.1999.9900.
32. **Tiscornia G, Singer O, Verma IM.** 2006. Production and purification of lentiviral vectors. Nat Protoc **1:**241–245. http://dx.doi.org/10.1038/nprot.2006.37.
33. **Bandyopadhyay C, Veettil MV, Dutta S, Chandran B.** 2014. p130Cas scaffolds the signalosome to direct adaptor-effector cross talk during Kaposi's sarcoma-associated herpesvirus trafficking in human microvascular dermal endothelial cells. J Virol **88:**13858–13878. http://dx.doi.org/10.1128/JVI.01674-14.
34. **Ansari MA, Dutta S, Veettil MV, Dutta D, Iqbal J, Kumar B, Roy A, Chikoti L, Singh VV, Chandran B.** 2015. Herpesvirus genome recognition induced acetylation of nuclear IFI16 is essential for its cytoplasmic translocation, inflammasome and IFN-beta responses. PLoS Pathog **11:**e1005019. http://dx.doi.org/10.1371/journal.ppat.1005019.
35. **Valiya Veettil M, Dutta D, Bottero V, Bandyopadhyay C, Gjyshi O, Sharma-Walia N, Dutta S, Chandran B.** 2014. Glutamate secretion and metabotropic glutamate receptor 1 expression during Kaposi's sarcoma-associated herpesvirus infection promotes cell proliferation. PLoS Pathog **10:**e1004389. http://dx.doi.org/10.1371/journal.ppat.1004389.
36. **Akula SM, Wang FZ, Vieira J, Chandran B.** 2001. Human herpesvirus 8 interaction with target cells involves heparan sulfate. Virology **282:**245–255. http://dx.doi.org/10.1006/viro.2000.0851.
37. **Mercer J, Helenius A.** 2009. Virus entry by macropinocytosis. Nat Cell Biol **11:**510–520. http://dx.doi.org/10.1038/ncb0509-510.
38. **Yan Q, Sun W, Kujala P, Lotfi Y, Vida TA, Bean AJ.** 2005. CART: an Hrs/actinin-4/BERP/myosin V protein complex required for efficient receptor recycling. Mol Biol Cell **16:**2470–2482. http://dx.doi.org/10.1091/mbc.E04-11-1014.
39. **Araki N, Hatae T, Yamada T, Hirohashi S.** 2000. Actinin-4 is preferentially involved in circular ruffling and macropinocytosis in mouse macrophages: analysis by fluorescence ratio imaging. J Cell Sci **113:**3329–3340.
40. **Veettil MV, Sharma-Walia N, Sadagopan S, Raghu H, Sivakumar R, Naranatt PP, Chandran B.** 2006. RhoA-GTPase facilitates entry of Kaposi's sarcoma-associated herpesvirus into adherent target cells in a Src-dependent manner. J Virol **80:**11432–11446. http://dx.doi.org/10.1128/JVI.01342-06.
41. **Kaibuchi K.** 1999. Regulation of cytoskeleton and cell adhesion by Rho targets. Prog Mol Subcell Biol **22:**23–38. http://dx.doi.org/10.1007/978-3-642-58591-3_2.
42. **Yoneda A, Multhaupt HA, Couchman JR.** 2005. The Rho kinases I and II regulate different aspects of myosin II activity. J Cell Biol **170:**443–453. http://dx.doi.org/10.1083/jcb.200412043.
43. **Frampton AR, Jr, Stolz DB, Uchida H, Goins WF, Cohen JB, Glorioso JC.** 2007. Equine herpesvirus 1 enters cells by two different pathways, and infection requires the activation of the cellular kinase ROCK1. J Virol **81:**10879–10889. http://dx.doi.org/10.1128/JVI.00504-07.
44. **Koivusalo M, Welch C, Hayashi H, Scott CC, Kim M, Alexander T, Touret N, Hahn KM, Grinstein S.** 2010. Amiloride inhibits macropinocytosis by lowering submembranous pH and preventing Rac1 and Cdc42 signaling. J Cell Biol **188:**547–563. http://dx.doi.org/10.1083/jcb.200908086.
45. **Tominaga T, Barber DL.** 1998. Na-H exchange acts downstream of RhoA to regulate integrin-induced cell adhesion and spreading. Mol Biol Cell **9:**2287–2303. http://dx.doi.org/10.1091/mbc.9.8.2287.
46. **Hooley R, Yu CY, Symons M, Barber DL.** 1996. G alpha 13 stimulates Na+-H+ exchange through distinct Cdc42-dependent and RhoA-dependent pathways. J Biol Chem **271:**6152–6158. http://dx.doi.org/10.1074/jbc.271.11.6152.
47. **Schwartz MA, Lechene C, Ingber DE.** 1991. Insoluble fibronectin activates the Na/H antiporter by clustering and immobilizing integrin alpha 5 beta 1, independent of cell shape. Proc Natl Acad Sci U S A **88:**7849–7853. http://dx.doi.org/10.1073/pnas.88.17.7849.
48. **Komada M, Soriano P.** 1999. Hrs, a FYVE finger protein localized to early endosomes, is implicated in vesicular traffic and required for ventral folding morphogenesis. Genes Dev **13:**1475–1485. http://dx.doi.org/10.1101/gad.13.11.1475.
49. **Welsch S, Habermann A, Jager S, Muller B, Krijnse-Locker J, Krausslich HG.** 2006. Ultrastructural analysis of ESCRT proteins suggests a role for endosome-associated tubular-vesicular membranes in ESCRT function. Traffic **7:**1551–1566. http://dx.doi.org/10.1111/j.1600-0854.2006.00489.x.
50. **Shibasaki F, Fukami K, Fukui Y, Takenawa T.** 1994. Phosphatidylinositol 3-kinase binds to alpha-actinin through the p85 subunit. Biochem J **302:**551–557. http://dx.doi.org/10.1042/bj3020551.
51. **Sharma-Walia N, Naranatt PP, Krishnan HH, Zeng L, Chandran B.** 2004. Kaposi's sarcoma-associated herpesvirus/human herpesvirus 8 envelope glycoprotein gB induces the integrin-dependent focal adhesion kinase-Src-phosphatidylinositol 3-kinase-rho GTPase signal pathways and cytoskeletal rearrangements. J Virol **78:**4207–4223. http://dx.doi.org/10.1128/JVI.78.8.4207-4223.2004.
52. **Bishop AL, Hall A.** 2000. Rho GTPases and their effector proteins. Biochem J **348:**241–255. http://dx.doi.org/10.1042/bj3480241.
53. **Kimura K, Ito M, Amano M, Chihara K, Fukata Y, Nakafuku M, Yamamori B, Feng J, Nakano T, Okawa K, Iwamatsu A, Kaibuchi K.** 1996. Regulation of myosin phosphatase by Rho and Rho-associated kinase (Rho-kinase). Science **273:**245–248. http://dx.doi.org/10.1126/science.273.5272.245.
54. **Morelli A, Chiozzi P, Chiesa A, Ferrari D, Sanz JM, Falzoni S, Pinton P, Rizzuto R, Olson MF, Di Virgilio F.** 2003. Extracellular ATP causes ROCK I-dependent bleb formation in P2X7-transfected HEK293 cells. Mol Biol Cell **14:**2655–2664. http://dx.doi.org/10.1091/mbc.02-04-0061.
55. **Sebbagh M, Renvoize C, Hamelin J, Riche N, Bertoglio J, Breard J.** 2001. Caspase-3-mediated cleavage of ROCK I induces MLC phosphorylation and apoptotic membrane blebbing. Nat Cell Biol **3:**346–352. http://dx.doi.org/10.1038/35070019.